Transient deformation of elastic capsules in shear flow: Effect of membrane bending stiffness

Y. Sui,[1] Y. T. Chew,[1] P. Roy,[2] X. B. Chen,[1] and H. T. Low[2,*]

[1]*Department of Mechanical Engineering, National University of Singapore, 9 Engineering Drive 1, Singapore 117576*

[2]*Division of Bioengineering, National University of Singapore, 9 Engineering Drive 1, Singapore 117576*

(Received 21 November 2006; revised manuscript received 3 April 2007; published 5 June 2007)

The transient deformation of liquid capsules enclosed by elastic membranes with bending rigidity in shear flow has been studied numerically, using an improved immersed boundary-lattice Boltzmann method. The purpose of the present study is to investigate the effect of interfacial bending stiffness on the deformation of such capsules. Bending moments, accompanied by transverse shear tensions, usually develop due to a preferred membrane configuration or its nonzero thickness. The present model can simulate flow induced deformation of capsules with arbitrary resting shapes (concerning the in-plane tension) and arbitrary configurations at which the bending energy has a global minimum (minimum bending-energy configurations). The deformation of capsules with initially circular, elliptical, and biconcave resting shapes was studied; the capsules' minimum bending-energy configurations were considered as either uniform-curvature shapes (like circle or flat plate) or their initially resting shapes. The results show that for capsules with minimum bending-energy configurations having uniform curvature (circle or flat plate), the membrane carries out tank-treading motion, and the steady deformed shapes become more rounded if the bending stiffness is increased. For elliptical and biconcave capsules with resting shapes as minimum bending-energy configurations, it is quite interesting to find that with the bending stiffness increasing, the capsules' motion changes from tank-treading mode to flipping mode, and resembles Jeffery's flipping mode at large bending stiffness.

DOI: 10.1103/PhysRevE.75.066301 PACS number(s): 47.55.−t

I. INTRODUCTION

The deformation of a liquid capsule enclosed by a thin elastic or incompressible membrane in simple shear flow has been studied by many researchers in cellular biology, bioengineering, and chemical engineering. It is important not only in fundamental research, but also in medical and industrial applications. For example, in blood diseases like cerebral malaria and sickle cell anemia, the red blood cells lose their ability to deform and often block the capillaries due to the membranes becoming stiffer. To design clinical therapies for such blood diseases, it is needed to understand how the interfacial mechanical properties affect the deformation of cells under flow. The capsule deformation is also important in other areas, such as microencapsulation, to design capsules with desired properties.

The dynamic motion of an elastic capsule under simple shear flow has been studied experimentally [1–4], theoretically [5–8], and numerically [9–17]. Previous researchers have found that there are mainly three types of motion: a steady mode in which the capsule deforms to a stationary configuration with the membrane rotating around the internal liquid (tank treading), and an unsteady mode in which the capsule tumbles continuously. The transition from tank treading mode to flipping mode due to increasing the viscosity of internal fluid has been studied in Refs. [7,11,13,14]; the mode transition due to increasing the viscosity of membrane has been studied in Refs. [15,16]. Recently, Misbah [8] has theoretically predicted a new unsteady mode under the condition that the viscosity contrast of the internal and the external fluids is large. In this mode the capsule inclination undergoes oscillation around the flow while the shape executes breathing dynamics. This vacillating-breathing mode coexists with the tumbling mode.

For liquid filled capsules enclosed by an elastic membrane, flow induced deformation causes the development of not only in-plane elastic tensions, but also bending moments accompanied by transverse shear tensions. The interfacial bending moments develop physically due to the nonzero membrane thickness; the bending moments may also be generated because the membrane has a preferred configuration due to its certain structure. The bending moments are expressed by a constitutive law which involves the instantaneous Cartesian curvature tensor, curvature of the minimum bending-energy configuration, and the bending modulus. The bending modulus is generally independent of the in-plane elasticity modulus, and describes the flexural stiffness of the membrane.

For fluid capsules enclosed by a lipid-bilayer membrane, such as red blood cells, the bending stiffness has been found quite important in determining the equilibrium configuration and shape oscillations [18,19]. For nonequilibrium conditions such as capsules under flow, membrane bending rigidity also plays a significant role in avoiding the development of wrinkling and folding. For capsules whose membrane has a preferred configuration, it can be expected that bending stiffness will ensure that the capsule shape should not deviate greatly from its preferred profile. It is thus meaningful to investigate the effect of bending stiffness on the flow-induced deformation of liquid filled capsules enclosed by an elastic membrane. However, this effect has not been explored much and most previous studies neglected bending resistance. A numerical study of Pozrikidis [12] showed that bending stiffness has a significant effect on the steady configuration of elastic capsules in simple shear flow. However,

*Corresponding author; FAX: (65)-67791459; Email address: mpelowht@nus.edu.sg

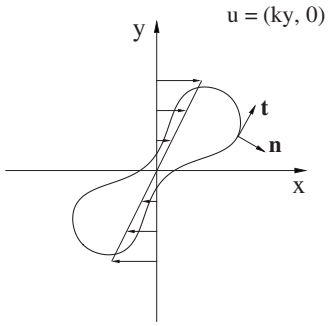

FIG. 1. Schematic illustration of a 2D capsule in simple shear flow.

an important restriction was the requirement that the minimum bending-energy shape has uniform curvature. So far, there is no study on the transient deformation of elastic capsules whose minimum bending-energy configuration has nonuniform curvature.

In the present study, the transient deformation of two-dimensional (2D) elastic capsules, filled with a Newtonian liquid similar to that outside, is studied numerically under a simple shear flow condition. The purpose of the present study is to investigate the effect of membrane preferred minimum bending-energy configurations (with uniform or nonuniform curvature) and interfacial bending stiffness on the deformation of such capsules. One must acknowledge that the 2D model is a large simplification; however, previous studies [10,13,14] have provided sufficient grounds which show that the 2D study maintains most common features of the 3D capsule motion; for example, the transition from tank treading mode to flipping mode.

The present study is based on the immersed boundary-lattice Boltzmann method which was proposed by Feng and Michaelides [20] to study particulate flow. It combines the immersed boundary method [21,22] with the lattice Boltzmann method [23–25] and keeps the merits of both methods. Recently, the present authors Sui *et al.* [17,26] improved this method by employing the multiblock strategy of Yu [27]. The computational domain is divided into blocks with different mesh resolutions, and fine mesh only covers the region near the moving boundaries. This has substantially improved the accuracy and efficiency of the simulation.

In the present study, the simulation of capsules deformation is based on the improved approach [26]. The flow field is solved by the lattice Boltzmann method, the fluid-capsule interaction is solved by the immersed boundary method, and the multiblock strategy is used to refine the mesh around the deforming capsule. The present model has been validated in a previous study [17], in which the bending stiffness is neglected.

II. MODEL AND METHOD

A. Interfacial mechanics

In the present study, the deformation of a 2D capsule is considered to be subjected to the two-dimensional incident shear flow along the x axis $\mathbf{u}=(ky,0)$ as illustrated in Fig. 1. The unit tangent vector $\mathbf{t}$ is pointing in the direction of increasing arc length and $\mathbf{n}$ is the unit normal vector pointing into the ambient fluid.

During the capsule deformation, the velocity across the interface is continuous in order to satisfy the nonslip condition. But there is a jump of the interfacial tension $\Delta\mathbf{F}$, which is in the form of [28]

$$\Delta\mathbf{F} = \Delta F^n\mathbf{n} + \Delta F^t\mathbf{t} = -\frac{d\mathbf{T}}{dl} = -\frac{d}{dl}(\tau\mathbf{t} + q\mathbf{n}), \tag{1}$$

where $\mathbf{T}$ is the membrane tension, consisting of the in-plane tension τ and transverse shear tension q. The in-plane tension τ is obtained from the membrane's constitutive law. In the present study, Hooke's law is employed due to its simplicity; however, it is sufficient to take deformability into account. It has the form

$$\tau = E\left(\frac{\partial l(t)}{\partial l_0} - 1\right), \tag{2}$$

where E represents the interfacial elasticity modulus, $l(t)$ is the membrane length at time t, and l_0 is the unstressed membrane length. The transverse shear tension q is expressed in terms of bending moment m as follows:

$$q = \frac{dm}{dl}. \tag{3}$$

The bending moment is given by

$$m = E_B[\kappa(l) - \kappa_0(l)], \tag{4}$$

where E_B is the bending modulus, $\kappa(l)$ is the instantaneous membrane curvature, and $\kappa_0(l)$ is the curvature of membrane at minimum bending-energy configuration [29].

In the present simulation, there is no special constraint for the volume of the capsule. The results show that the volume change during capsule deformation is less than 0.1%.

Due to the small length scale (10^{-6}–10^{-5} m) of the capsule and the small surrounding fluid velocity (10^{-3}–10^{-2} m/s), the initial effect is neglected. Two dimensionless parameters are believed to play an essential role in determining the capsule deformation. One is the dimensionless shear rate G, which determines the relative importance of shearing and elasticity, in the form of

$$G = \frac{\mu k a}{E}, \tag{5}$$

where μ is the viscosity of the surrounding fluid, k is the shear rate, and the term a is the equivalent radius, in the form of $a=(\text{capsule area}/\pi)^{0.5}$. Another important parameter is the reduced ratio of bending to elasticity moduli, in the form of

$$E_b = \frac{E_B}{a^2 E}. \tag{6}$$

B. Numerical method

The present simulation is based on a hybrid method of Sui *et al.* [17,26]. The concept is based on introducing the im-

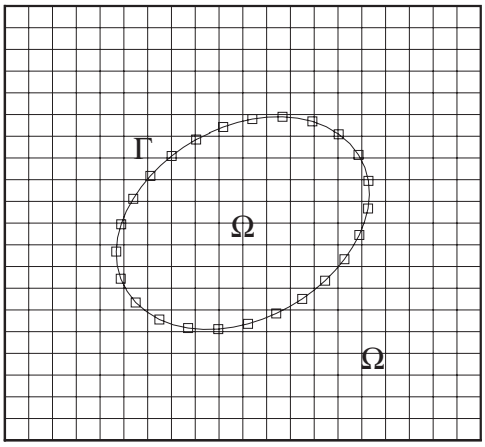

FIG. 2. Schematic illustration of a body whose boundary has been divided into Lagrangian nodes immersed in a Cartesian mesh.

mersed boundary method in the framework of the lattice Boltzmann model, and using multiblock strategy to refine the mesh near the moving boundary.

In the immersed boundary method of Peskin [21,22], a force density is distributed to the Cartesian mesh in the vicinity of the moving boundary in order to account for the effect of the boundary. To explain this method, consider a massless elastic capsule with boundary Γ immersed in the fluid domain Ω (see Fig. 2). The fluid domain Ω is represented by Eulerian coordinates $\mathbf{x}$, while the boundary of the capsule Γ, is represented by Lagrangian coordinates $\mathbf{s}$. Any position on the capsule membrane can be written as $\mathbf{X}(\mathbf{s},t)$. The term $\mathbf{F}(\mathbf{s},t)$ represents the membrane force density, which is a combination of the internal link force induced by deformation and the external force. The term $\mathbf{f}(\mathbf{s},t)$ represents the fluid body force density.

The nonslip boundary condition is satisfied by letting the flexible structure move at the same velocity as the fluid around it. That is,

$$\frac{\partial \mathbf{X}(\mathbf{s},t)}{\partial t} = \mathbf{u}(\mathbf{X}(\mathbf{s},t),t). \tag{7}$$

This motion will cause the capsule to deform. The boundary force density $\mathbf{F}(\mathbf{s},t)$ is obtained from the constitutive law of the capsule, and distributed to the fluid mesh points near it by a dirac delta function, written as follows:

$$\mathbf{f}(\mathbf{x},t) = \int_{\Gamma} \mathbf{F}(\mathbf{s},t)\,\delta[\mathbf{x} - \mathbf{X}(\mathbf{s},t)]d\mathbf{s}. \tag{8}$$

The same Dirac delta function is used to obtain the velocities of the Lagrangian nodes on the moving boundary. Details were given by Sui *et al.* [26].

The lattice Boltzmann method [23–25] is a kinetic-based approach for simulating fluid flows. It decomposes the continuous fluid flow into pockets of fluid particles which can only stay at rest or move to one of the neighboring nodes. In the present study, the immersed boundary method is combined with the lattice Boltzmann method. In order to solve the flow field with a force density, the lattice Boltzmann equation (LBE) must be modified. Several forms of LBE which can handle a force density have been proposed. Guo's approach [30] is more accurate for unsteady flow with force changing with time and space, in which the modified lattice Boltzmann equation is in the form of

$$f_i(\mathbf{x} + \mathbf{e}_i\Delta t, t + \Delta t) - f_i(\mathbf{x},t) = -\frac{1}{\tau}[f_i(\mathbf{x},t) - f_i^{eq}(\mathbf{x},t)] + \Delta t F_i, \tag{9}$$

where the term i is the velocity index; here the two-dimension and nine-velocity model is employed. The term $f_i(\mathbf{x},t)$ is the distribution function for particles with velocity $\mathbf{e}_i$ at position $\mathbf{x}$ and time t, Δt is the lattice time interval, $f_i^{eq}(\mathbf{x},t)$ is the equilibrium distribution function, and τ is the nondimensional relaxation time.

The equilibrium distribution function $f_i^{eq}(\mathbf{x},t)$ is in the form of

$$f_i^{eq} = E_i(\rho,\mathbf{u}), \tag{10}$$

with

$$E_i(\rho,\mathbf{u}) = \omega_i\rho\left[1 + \frac{\mathbf{e}\cdot\mathbf{u}}{c_s^2} + \frac{\mathbf{uu}:(\mathbf{e}_i\mathbf{e}_i - c_s^2\mathbf{I})}{2c_s^4}\right], \tag{11}$$

where ω_i is the weighing factor; it equals 4/9 for $i=0$, 1/9 for $i=1-4$, and 1/36 for $i=5-8$. The term c_s represents the sound speed, and equals $\Delta x/(\sqrt{3}\Delta t)$.

The relaxation time is related to the kinematic viscosity in the Navier-Stokes equation in the form of

$$\nu = \left(\tau - \frac{1}{2}\right)c_s^2\Delta t. \tag{12}$$

The forcing term F_i is in the form of

$$F_i = \left(1 - \frac{1}{2\tau}\right)\omega_i\left[\frac{\mathbf{e}_i - \mathbf{u}}{c_s^2} + \frac{(\mathbf{e}_i\cdot\mathbf{u})}{c_s^4}\mathbf{e}_i\right]\cdot\mathbf{f}. \tag{13}$$

Once the particle density distribution is known, the fluid density and momentum are calculated, using

$$\rho = \sum_i f_i, \quad \rho\mathbf{u} = \sum_i \mathbf{e}_i f_i + \frac{1}{2}\mathbf{f}\Delta t. \tag{14}$$

In the present paper, the multiblock strategy proposed by Yu [27] is employed. The computational domain is divided into blocks which are connected through the interface. On the interface between blocks, the exchange of variables follows a certain relation so that the mass and momentum are conserved and the stress is continuous across the interface.

Consider a two-block system to explain the idea of the multiblock method. The ratio of lattice space between the two blocks is defined as $m=\Delta x_c/\Delta x_f$, where Δx_c and Δx_f are the lattice space of the coarse and fine mesh blocks, respectively. For a given lattice space, the fluid viscosity can be obtained from Eq. (12). In order to keep a constant viscosity, the relaxation parameter τ_f in fine mesh and τ_c in coarse mesh, must satisfy the following relation:

$$\tau_f = \frac{1}{2} + m\left(\tau_c - \frac{1}{2}\right). \tag{15}$$

The variables and their derivatives on the grid must be continuous across the block interface. To keep this continuity, the relation of the density distribution function in the neighboring blocks is proposed as

$$\tilde{f}_i^c = f_i^{eq,f} + m\frac{\tau_c - 1}{\tau_f - 1}[\tilde{f}_i^f - f_i^{eq,f}],$$

$$\tilde{f}_i^f = f_i^{eq,c} + \frac{\tau_f - 1}{m(\tau_c - 1)}[\tilde{f}_i^c - f_i^{eq,c}], \tag{16}$$

where $\tilde{f}_i$ is the postcollision density distribution function.

As on each block the fluid particle has the same streaming velocity, the computation marches m steps on the fine-mesh block for every one step on the coarse-mesh block. On the interface, spatial and temporal interpolation of $\tilde{f}_i^f$ is needed to complete the information exchange. A symmetric, cubic spine fitting is employed for spatial interpolation and a three-point Lagrangian formula is used for temporal interpolation. The details of these interpolations are as given by Yu [27].

In the computation, a two-grid system is employed. The lattice space ratio between coarse and fine grids equals two. The elastic capsule is immersed in the fine mesh block. The present procedure for multiblock computation was given in detail by Sui *et al.* [26]. The numerical model has been validated in a previous study of Sui *et al.* [17] for the reduced bending modulus $E_b=0$ under various dimensionless shear rates.

III. RESULTS AND DISCUSSIONS

A. Initially circular capsules

The deformation of capsules with initially circular shape in simple shear flow is studied. The initial shape is also the resting shape concerning the in-plane tension. The results presented in this section correspond to capsules whose initial shape is also the minimum bending-energy profile. Capsules with flat minimum bending-energy shape are found to behave in a similar way.

In the present study, all variables are normalized by the characteristic length $2a$, velocity $2ka$, and time $1/k$. The Reynolds number based on the above characteristic length and velocity was 0.05. The membrane shear elasticity modulus was varied so that different dimensionless shear rates were obtained and studied. The computational domain ranged from 0 to $16a$ in both the x axis and the y axis. Numerical experiment showed that the size of this computational domain is large enough to neglect the boundary effect. The capsule was at the center of the domain, and its membrane was equally discretized into 160 Lagrangian nodes. The fine mesh block covered from $5a$ to $11a$ in both axes. The other area was covered with coarse mesh. The grid resolutions in fine and coarse block were $\Delta x_f = \Delta y_f = 0.05a$ and $\Delta x_f = \Delta y_f = 0.1a$, respectively. Grid-independent study showed that this mesh density was sufficient. The characteristic velocity was set to be 1×10^{-4}, so that the relaxation parameters in coarse block and fine block were 0.62 and 0.74, respectively.

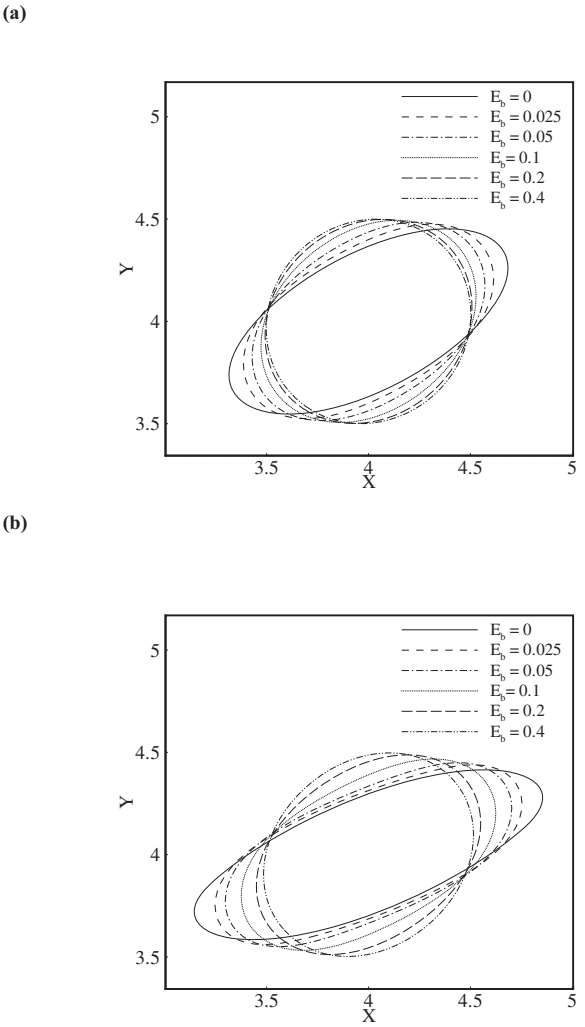

FIG. 3. Contours of steady deformed capsules with circular initial shape for various bending modulus at dimensionless shear rate: (a) $G=0.04$ and (b) $G=0.125$.

The present results show that the capsules deform to steady shapes and then the membrane rotates around the liquid inside (tank-treading motion). Figure 3(a) presents a family of configurations of steady deformed capsules for reduced bending modulus $E_b=0-0.4$ at the dimensionless shear rate $G=0.04$. As expected, the effect of bending stiffness is apparent. It restricts the global deformation of capsules, and locally prevents the development of highly curved shapes at the two tips. With the increase of the bending modulus, the shapes of the steady deformed capsules become closer to a circle and the orientations become less aligned with the flow direction. If the shear rate is higher, as shown in Fig. 3(b) for $G=0.125$, it is seen that the capsules are more deformed for the same reduced bending modulus.

To quantitatively illustrate the effect of bending stiffness on the capsules deformation, the temporal evolution of the Taylor deformation parameter and inclination angle (with respect to the x axis) are presented in Fig. 4, for $G=0.04$ and

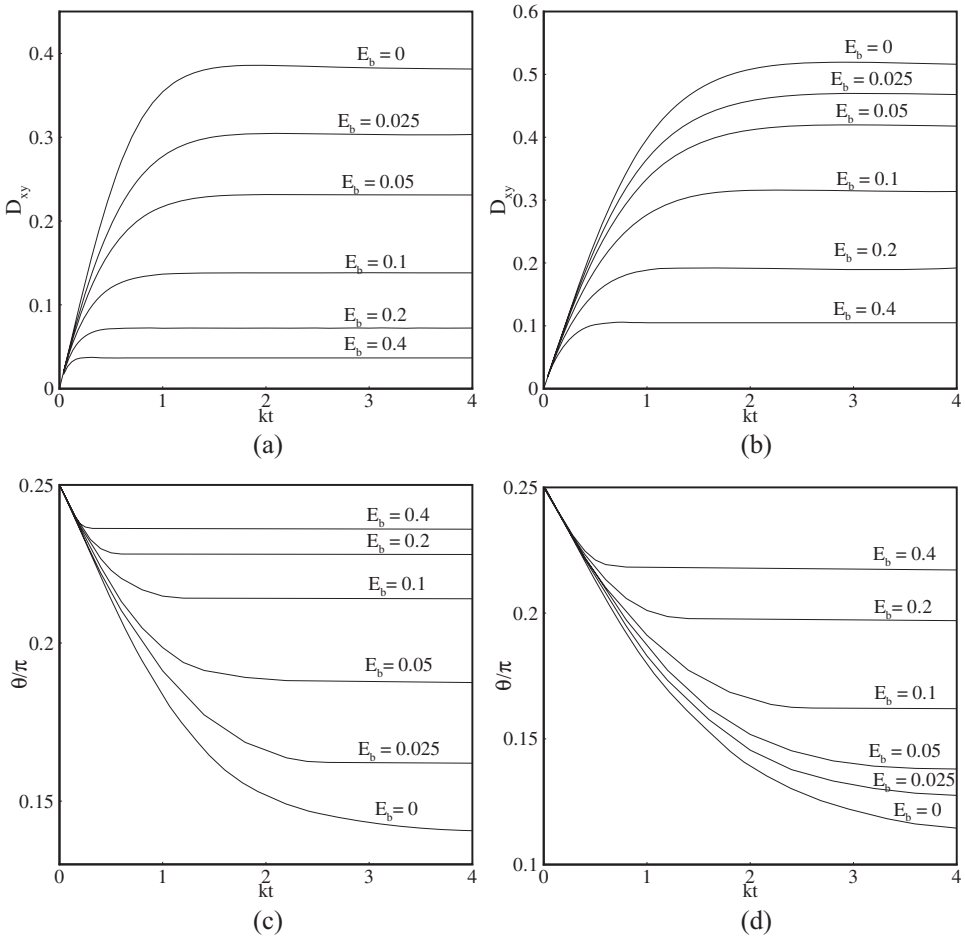

FIG. 4. Temporal evolution of Taylor deformation parameter for (a) $G=0.04$ and (b) $G=0.125$; inclination angle for (c) $G=0.04$ and (d) $G=0.125$.

0.125. The Taylor deformation parameter is defined as $D_{xy}=(L-B)/(L+B)$, where L and B are the length and width of a capsule. The quantitative results confirm that increased bending stiffness reduces the capsule deformation and makes it less aligned with the flow. It is also seen that the time taken to achieve steady shape is shorter under a lower dimensionless shear rate or higher reduced bending modulus. That is because the capsule only needs to deform a little to generate enough elastic force to balance the viscous shear force.

After the capsule deforms to a steady configuration, its membrane rotates around the liquid inside with period T. The normalized tank-treading frequency $f=4\pi/(kT)$ is presented in Fig. 5 for various bending modulus at $G=0.04$ and 0.125. It is seen that, with an increasing bending modulus, the dimensionless frequency asymptotically approaches towards the value of unity, corresponding to that of a solid circular cylinder in simple shear flow.

B. Initially elliptical capsules

In this section, the deformation of initially elliptical capsules, with a semimajor to semiminor axes ratio of 2:1 and equivalent radius a, is simulated under the dimensionless shear rate $G=0.04$ and 0.125. The capsules are initially unstressed concerning the in-plane tension. Various resting configurations concerning the bending moments are considered: uniform curvature shapes (circle and flat plate) and nonuniform curvature shape (the initially elliptical configuration). The computational domain, block system, mesh resolutions, and characteristic scales are the same as that in the previous section.

Consider first the minimum bending-energy shape having uniform curvature shape which is circular. The area of the circle is the same as that of the initially elliptical capsule. Figures 6(a) and 6(b) present the configurations of steady deformed capsules with the reduced bending modulus in-

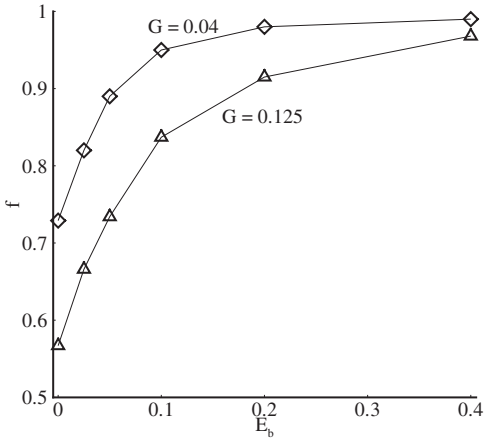

FIG. 5. The normalized tank-treading frequency for various reduced bending modulus at $G=0.04$ and 0.125.

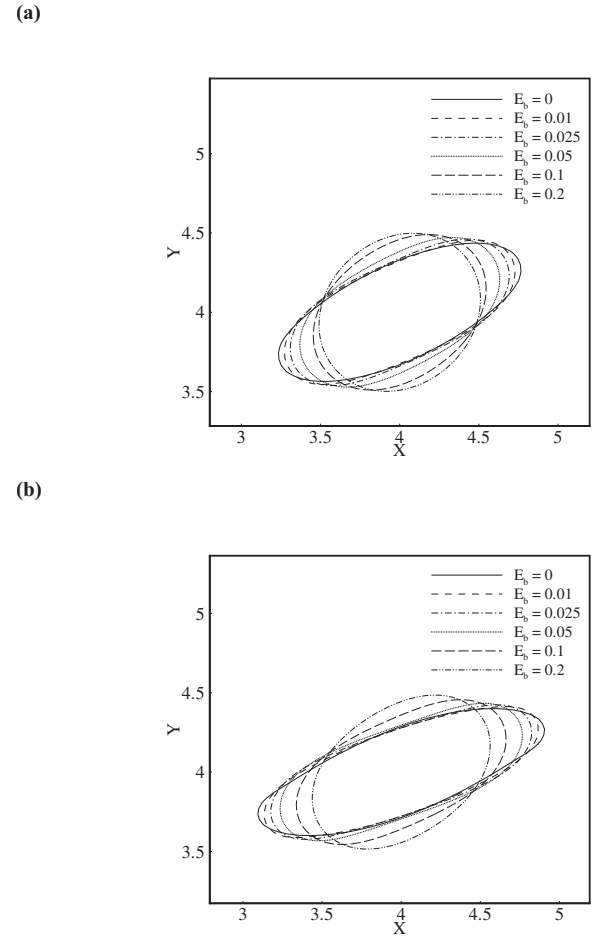

FIG. 6. Configurations of steady deformed capsules with elliptical initial shape and various bending modulus at dimensionless shear rate: (a) $G=0.04$ and (b) $G=0.125$.

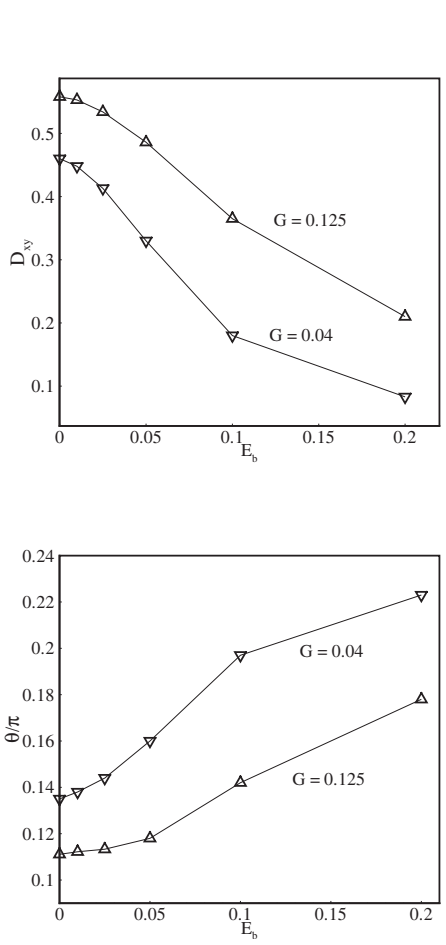

FIG. 7. Steady (a) Taylor deformation parameters and (b) inclination angles of capsules with different reduced bending modulus at $G=0.04$ and 0.125.

creasing up to 0.2, at the dimensionless shear rate $G=0.04$ and 0.125, respectively. The overall deformation of the capsules is quite similar to that of the initially circular capsules. As the bending modulus increases, the steady configurations of capsules tend to become circular. Figures 7(a) and 7(b) present the steady Taylor deformation parameters and inclination angles of capsules with different bending modulus ratios. It is shown from the results that as E_b increases, the Taylor deformation parameter decreases while the inclination angle increases monotonically. The minimum bending-energy shape having uniform curvature, which is flat, has also been studied. It was found that they behave in a similar way.

For a capsule membrane with a certain structure, composed, for example, of polymeric or proteinic networks, the membrane may prefer a certain resting configuration concerning the bending moments, due to the membrane structure. This preferred minimum bending-energy configuration may have nonuniform curvature. However, the transient deformation of elastic capsules with minimum bending-energy configuration having nonuniform curvature has not been studied so far. In this section, the capsules' initially elliptical shape is chosen as the minimum bending-energy configuration. The present membrane model is able to describe the in-plane elasticity and bending moments, but it does not represent the polymerized structures of the membrane.

Without bending stiffness, it is well known that a capsule will deform to a stationary shape with a finite inclination angle, then the membrane rotates around the liquid inside, as presented in Fig. 8(a). When there is bending stiffness, it will try to keep the instantaneous curvature of the capsule akin to its initial curvature.

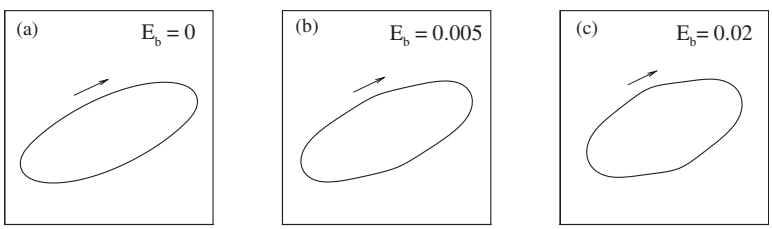

FIG. 8. Tank-treading motion of capsules with the elliptical initial shape as the minimum bending-energy configuration at different bending modulus at $G=0.04$.

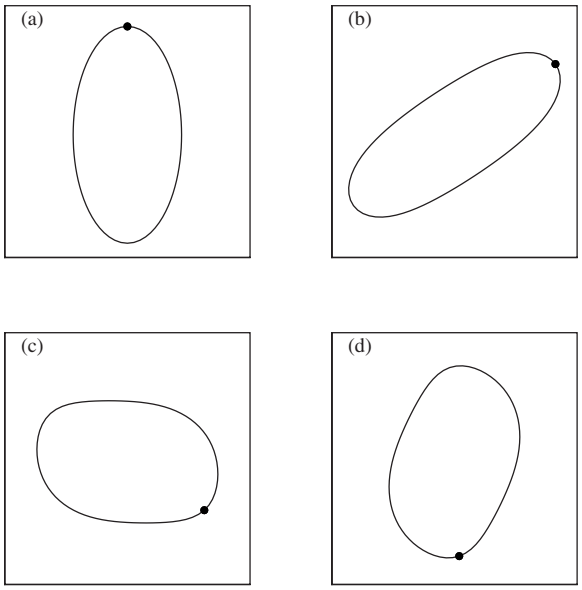

FIG. 9. Rotating and deforming of an elliptical capsule with $E_b=0.06$ at $G=0.04$. Corresponding dimensionless times are $kt=0$ (a), 1.6 (b), 6.4 (c), and 8 (d).

From the present results, it is interesting to find that with a finite but small bending modulus, the membrane still carries out tank-treading motion. However, two protrusions develop on the membrane and rotate around the liquid inside, as presented in Figs. 8(b) and 8(c) for $E_b=0.005$ and 0.02, respectively. The animation of the capsule contours shows that the capsule inclination is undergoing periodic oscillation while the membrane with protrusions rotates. These observations are different from that of a capsule without bending stiffness or with a minimum bending-energy shape of uniform curvature. As the bending modulus increases, the protrusions become larger (see Fig. 8), and so does the oscillation amplitude of the capsule's inclination angle.

When the reduced bending modulus reached 0.06, the motion of the capsule has changed from tank-treading mode to flipping mode accompanied with periodic deformation. Figure 9 presents a series of capsule contours for $E_b=0.06$ and $G=0.04$, at the dimensionless time $kt=0$, 1.6, 6.4, and 8. The symbol ● represents the same Lagrangian node on the membrane. From the results, it is seen that the capsule is undergoing flipping motion. It is elongated or compressed by the shear flow periodically.

With a further increase in bending stiffness the flipping motion continues, but the capsule is hardly deformed and behaves like a rigid body. Figure 10 presents the capsule contour for $E_b=0.4$ and $G=0.04$ at $kt=0$, 2, and 6.4. It is seen that the capsule tumbles without visible shape changes.

Figure 11 presents the temporal evolution of the capsule inclination angle for various bending modulus at $G=0.04$. It is seen that without bending stiffness ($E_b=0$), a steady tank-treading mode is achieved; with a finite but small bending stiffness ($E_b=0.005$, 0.02, and 0.04), the capsule's orientation undergoes oscillation with amplitude increasing as the bending modulus increases. Further increasing the bending rigidity ($E_b=0.06$ and 0.4) causes the mode transition; that is, the oscillation amplitude is larger than π. Figure 11 shows

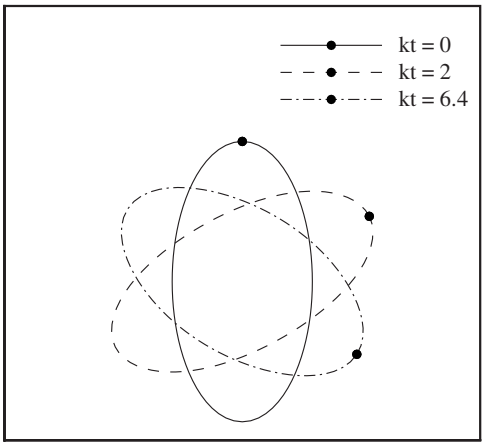

FIG. 10. Rotating and deforming of an elliptical capsule with $E_b=0.4$ at $G=0.04$.

that the transition happens between $E_b=0.04$ and 0.06. For a rigid ellipse rotating in two-dimensional shear flow at vanishing Reynolds number, its orbit can be predicted by Jeffery's theory [31]. The angular rotation is given by

$$\theta = \tan^{-1}\left(r \tan \frac{rkt}{1+r^2}\right), \tag{17}$$

where r is the aspect ratio, which equals 2 in the present study. Jeffery's solution is plotted in Fig. 11. For $E_b=0.06$, the capsule is undergoing flipping motion. However, due to its deformability, the result departs largely from Jeffery's theory. For $E_b=0.4$ when the deformation of the capsule is small, reasonable quantitative agreement is observed, which confirms that the capsule tumbles like a rigid body.

Simulation for capsules with various bending modulus for dimensionless shear rate $G=0.125$ has also been carried out. It was found that the behavior of the capsules is similar to that for $G=0.04$. However, the critical bending modulus for modes transition is higher.

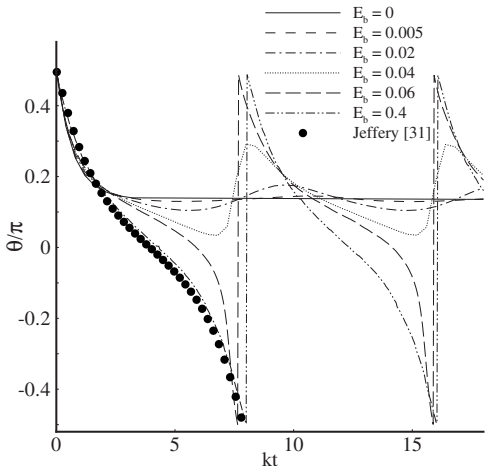

FIG. 11. Evolution of inclination angle of capsules with the elliptical initial shape as the minimum bending-energy configuration at $G=0.04$.

Through the above observations, it is found that with the bending stiffness increasing, the motion of a capsule can be divided into four sequential stages: (1) steady tank-treading mode (at zero bending stiffness), (2) tank treading with orientation oscillation and shape deformation (at finite but small bending stiffness), (3) tumbling with periodic shape deformation (at moderate bending stiffness), and (4) tumbling like a rigid body (at large bending stiffness). The motion of the capsule at stage 2 seems similar to the "vacillating-breathing" mode, which is theoretically predicted by Misbah [8].

Without bending stiffness, the shear elasticity of the capsule membrane can only resist membrane in-plane stretching. Thus the shear torque can be easily transferred to the membrane, which will lead to steady tank-treading motion. However, transition to tumbling may be triggered for cases where (i) the viscosity contrast is large enough [7,11,13,14], and (ii) the membrane viscosity is increased [15,16]. In both cases due to the fact that the viscosity increases, the transfer of shear torque to the membrane becomes more and more difficult; and then the capsule would behave like a solid body which undergoes tumbling.

In this section, the elliptical capsule's initial shape is the minimum bending-energy shape. Due to the bending stiffness, the membrane's instantaneous curvature $\kappa(l)$ must keep akin to $\kappa_0(l)$, the curvature of the elliptical shape. This will restrict the deformability of the capsule. In shear flow, with the bending stiffness increasing, it becomes more and more difficult for the capsule to deform. Thus it becomes more difficult for the shear torque to be transferred to the membrane; and then the capsule will undergo flipping motion. With a large bending stiffness, the capsule is hardly able to deform and thus flips like a rigid body.

C. Initially biconcave capsules

The biconcave capsule has an initial shape [32] given by

$$x = a\alpha \sin \chi,$$

$$y = a\frac{\alpha}{2}(0.207 + 2.003 \sin^2 \chi - 1.123 \sin^4 \chi)\cos \chi, \quad (18)$$

where α is the cell radius ratio which equals 1.39 for a red blood cell, and the parameter χ ranges from -0.5π to 1.5π. This shape is the cross section of a three-dimensional red blood cell with equivalent radius a. Its two-dimensional equivalent radius is $0.74a$. The capsules are initially unstressed concerning the in-plane tension. Various minimum bending-energy configurations, including uniform curvature shapes (circle and flat plate) and nonuniform curvature shape (the initially biconcave configuration) are studied. The computational domain, block system, and mesh resolutions are the same as that in previous sections. The characteristic length is the equivalent diameter of the biconcave capsule, which equals $1.48a$. The characteristic velocity is $1.48ka$ and the Reynolds number is at 0.027.

The deformation of capsules with circular minimum bending-energy shape is first considered. The area of the circle is the same as that of the biconcave capsule. Figure 12 presents the configurations of steady deformed capsules with the reduced bending modulus increasing up to 0.1, at the dimensionless shear rate $G=0.025$. The rounding effect is apparent. As the bending modulus increases, the circularity of the steady deformed capsules increases. Capsules with flat resting shape concerning the bending moments have also been studied. A similar phenomenon was observed.

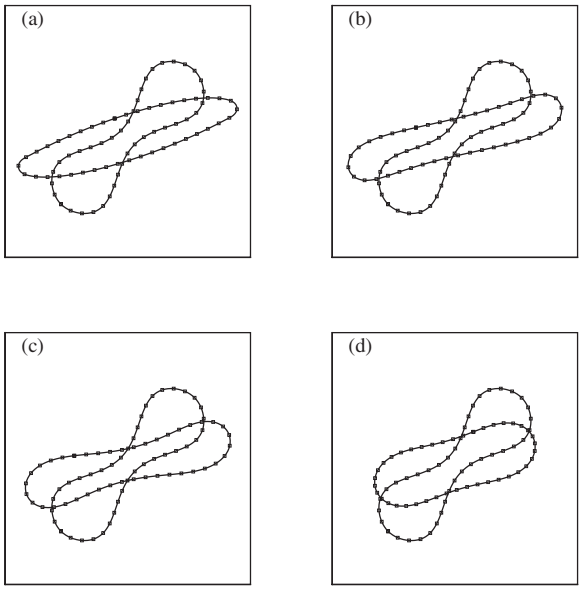

FIG. 12. Equilibrium shapes of biconcave capsules with reduced bending modulus $E_b=0$ (a), 0.005 (b), 0.02 (c), and 0.1 (d) at $G=0.025$.

Also studied is the deformation of capsules with the initially biconcave shape as the minimum bending-energy configuration. Figure 13 presents the capsule profiles at different times for $E_b=0.015$ and $G=0.025$. From the results it is seen that the capsule still carries out motion of the tank-treading mode. Protrusions develop along the membrane and rotate around the internal liquid. The animation of the capsule configurations shows that the capsule inclination is undergoing periodic oscillation while the membrane rotates. The oscillation amplitude increases with the bending modulus increas-

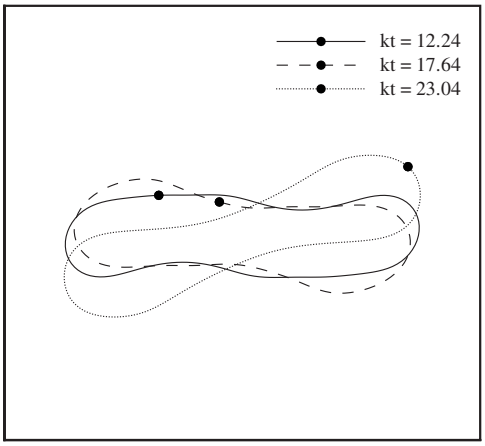

FIG. 13. Tank treading and deforming of a biconcave capsule with $E_b=0.015$ at $G=0.025$.

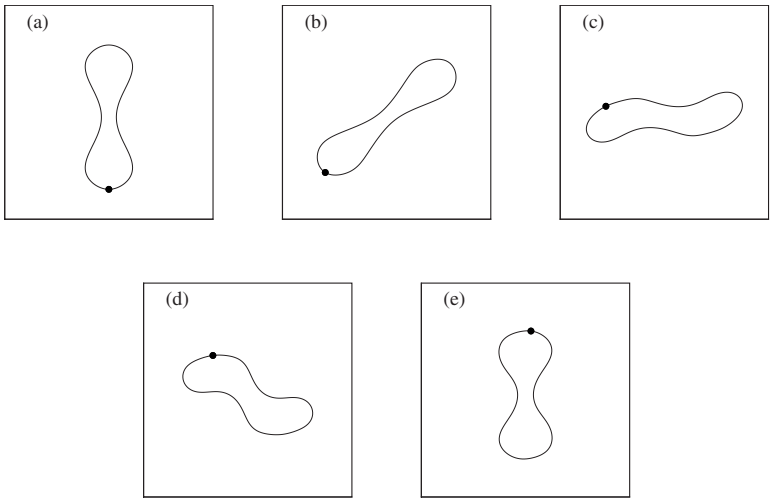

FIG. 14. Rotating and deforming of a biconcave capsule with $E_b=0.02$ at $G=0.025$. Corresponding dimensionless times are $kt=0$ (a), 1.26 (b), 7.38 (c), 14.22 (d), and 15.66 (e).

ing and finally the motion changes to flipping mode.

Figure 14 presents a family of capsule contours for $E_b=0.02$ at the dimensionless time $kt=0$, 1.26, 7.38, 14.22, and 15.66. The results show that the capsule is tumbling continuously. The animation of the capsule contours shows that the flipping motion is accompanied by periodic deformation. The capsule is elongated [illustrated in Fig. 14(b)] or compressed [illustrated in Fig. 14(d)] by the shear flow. Further increasing the bending stiffness makes the capsule carry out rigid-body-like flipping motion, which resembles Jeffery's mode, as illustrated in Fig. 15 for $E_b=0.2$.

Figure 16(a) presents the temporal evolution of the capsule inclination angle for various bending modulus at $G=0.025$. It is seen that for low bending modulus, the inclination is undergoing small oscillations. The oscillation amplitude increases as the bending modulus increases, and finally causes the change from tank treading to flipping modes. The result shows that this transition happens between $E_b=0.015$ and 0.02. During the flipping motion, the capsule rotates faster when perpendicular to the flow and slower when aligned with the flow direction. For $E_b=0.2$ in which the deformation of the capsule is small, the orbit of the capsule is compared with Jeffery's theory. In Eq. (17), the aspect ratio is determined following the approach in Refs. [1,11].

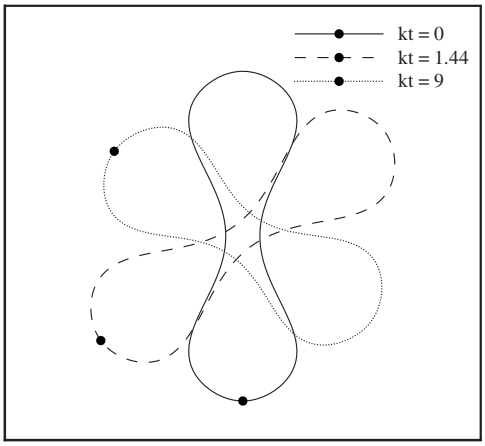

FIG. 15. Rotating and deforming of a biconcave capsule with $E_b=0.2$ at $G=0.025$.

That is, it is chosen so that the numerical flipping period matches that predicted by theory. Satisfactory quantitative agreement is observed in Fig. 16(a).

It has been shown in previous studies [10,17] that a biconcave capsule achieves a steady tank-treading mode without bending stiffness. In the present section, a four-stage motion, similar to that in Sec. III B, is found for a biconcave

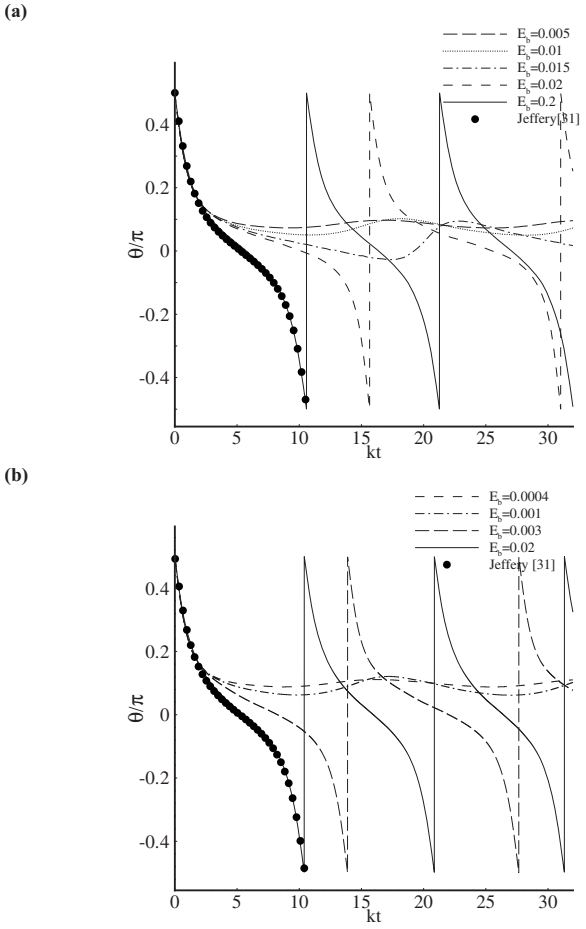

FIG. 16. Evolution of inclination angle of capsules with the biconcave initial shape as the minimum bending-energy configuration at (a) $G=0.025$ and (b) $G=0.0025$.

capsule with various bending stiffness. The physical mechanism should also be the same.

It is well known that the red blood cell membrane is strongly resistant to area dilatation. The membrane model employed here does allow area dilatation. However, the present methodology allows incorporation of incompressible membrane models. With the Hooke's law used in the present study, by increasing the membrane elasticity, a case with membrane incompressibility can be approximated. This case was studied with $G=0.0025$ under various bending stiffness. The maximum membrane area change was within 0.5%. The temporal evolution of the capsule inclination angle is presented in Fig. 16(b). The capsule motion is closely similar to that for $G=0.025$ and so is the transition to flipping mode. However, the critical bending modulus for motion transition is lower.

IV. CONCLUSION

The effect of interfacial bending stiffness on the deformation of liquid capsules enclosed by elastic membranes in shear flow has been studied numerically, using an improved immersed boundary-lattice Boltzmann method. Initially, circular, elliptical, and biconcave capsules with various minimum bending-energy shapes, including circular, flat plate, or their initially resting shapes have been studied. The results show that for capsules with minimum bending-energy configurations having uniform curvature (circular, flat plate), the steady deformed shapes are more rounded with increasing bending stiffness. For initially elliptical and biconcave capsules with their initial configurations as the minimum bending-energy shapes, it is interesting to find that with the bending stiffness increasing, the capsules' behavior changes from tank-treading mode to flipping mode, and achieves Jeffery's flipping mode with a large bending stiffness. The present study shows that, besides viscosity ratio and membrane viscosity, the membrane bending stiffness may be another factor which can lead to the transition of a capsule's motion from tank treading to flipping.

[1] H. L. Goldsmith and J. Marlow, Proc. R. Soc. London, Ser. B **182**, 351 (1972).
[2] T. M. Fischer, M. Stöhr-Liesen, and H. Schmid-Schönbein, Science **202**, 894 (1978).
[3] S. Chien, Annu. Rev. Physiol. **49**, 177 (1987).
[4] K. H. de Haas, C. Blom, D. van den Ende, M. H. G. Duits, and J. Mellema, Phys. Rev. E **56**, 7132 (1997).
[5] D. Barthès-Biesel, J. Fluid Mech. **100**, 831 (1980).
[6] D. Barthès-Biesel and J. M. Rallison, J. Fluid Mech. **113**, 251 (1981).
[7] S. R. Keller and R. Skalak, J. Fluid Mech. **120**, 27 (1982).
[8] C. Misbah, Phys. Rev. Lett. **96**, 028104 (2006).
[9] M. Kraus, W. Wintz, U. Seifert, and R. Lipowsky, Phys. Rev. Lett. **77**, 3685 (1996).
[10] H. Zhou and C. Pozrikidis, J. Fluid Mech. **283**, 175 (1995).
[11] S. Ramanujan and C. Pozrikidis, J. Fluid Mech. **361**, 117 (1998).
[12] C. Pozrikidis, J. Fluid Mech. **440**, 269 (2001).
[13] T. Biben and C. Misbah, Phys. Rev. E **67**, 031908 (2003).
[14] J. Beaucourt, F. Rioual, T. Séon, T. Biben, and C. Misbah, Phys. Rev. E **69**, 011906 (2004).
[15] H. Noguchi and G. Gompper, Phys. Rev. Lett. **93**, 258102 (2004).
[16] H. Noguchi and G. Gompper, Phys. Rev. E **72**, 011901 (2005).
[17] Y. Sui, Y. T. Chew, and H. T. Low, Int. J. Mod. Phys. C (to be published).
[18] R. Lipowsky, Nature (London) **349**, 475 (1991).
[19] *Foundations of Solid Mechanics*, edited by Y. C. Fung (Prentice-Hall, Englewood Cliffs, NJ, 1965).
[20] Z. G. Feng and E. E. Michaelides, J. Comput. Phys. **195**, 602 (2004).
[21] C. S. Peskin, J. Comput. Phys. **25**, 220 (1977).
[22] C. S. Peskin, J. Fourier Anal. Appl. **11**, 479 (2002).
[23] S. V. Lishchuk and C. M. Care, Phys. Rev. E **71**, 053201 (2005).
[24] X. L. Yin, D. L. Koch, and R. Verberg, Phys. Rev. E **73**, 026301 (2006).
[25] S. V. Lishchuk, I. Halliday, and C. M. Care, Phys. Rev. E **74**, 017701 (2006).
[26] Y. Sui, Y. T. Chew, P. Roy, and H. T. Low, Int. J. Numer. Methods Fluids **53**, 1727 (2007).
[27] D. Yu, R. Mei, and W. Shyy, Int. J. Numer. Methods Fluids **39**, 99 (2002).
[28] *Modeling and Simulation of Capsules and Biological Cells*, edited by C. Pozrikidis (Chapman & Hall/CRC, London, 2003).
[29] D. J. Steigmann and R. W. Ogden, Proc. R. Soc. London, Ser. A **453**, 853 (1997).
[30] Z. L. Guo, C. G. Zheng, and B. C. Shi, Phys. Rev. E **65**, 046308 (2002).
[31] J. B. Jeffery, Proc. R. Soc. London, Ser. A **102**, 161 (1922).
[32] C. Pozrikidis, Ann. Biomed. Eng. **31**, 1194 (2003).